Journal of Applied Sciences 9 (3): 438-448, 2009
ISSN 1812-5654

Experimental Study of Crack Growth Behavior and Fatigue Life of Spot Weld Tensile-Shear Specimens

M. Shariati and M.J. Maghrebi
Department of Mechanical, Shahrood University of Technology,
Daneshgah Blvd. Shahrood, Islamic Republic of Iran

Abstract: In this study, the experimental behaviors of the fatigue crack growth are studied and the fatigue lives of tensile-shear (TS) specimens are determined. To achieve this, many TS specimens are prepared by the welding mild steel sheets of 1 and 1.5 mm thickness and then tested under constant amplitude loading using a servo-hydraulic fatigue testing machine (INSTRON 8802). The fatigue crack growth and the crack length are measured simultaneously by an optical microscope with 100X magnification. The experimental results indicate that the fatigue life of specimens decreases with any increase in load level. Also the crack initiation and propagation firstly occurs in plate with less thickness. According to the experimental observations when a high level loading is applied to the spot weld joints, the nugget suddenly pull-out and cannot withstand the fatigue loading.

Key words: Spot weld, crack growth, fatigue life, tensile-shear specimens, crack propagation

INTRODUCTION

Spot welding is the simplest and the most commonly used technique in welding industries. In this type of welding, copper electrodes with smaller cross-section at the tip are used. The diameter of the welding point depends on the application and normally changes between 2 and 12 mm. After locating the workpiece, electrode is placed on it and the spot welding performed under a controlled current and pressure cycle. Then electrode opens and the workpiece is released. In Spot welding the deformation of metal under the electrode must be negligible. More than 2000 spot welding points are used for manufacturing of a typical car (Lin *et al*., 2002). Due to this reason the study of the crack growth behavior and the determination of the spot welding fatigue life have been always under a serious consideration by researchers. Investigators have tried to predict the fatigue life of spot welds by different experimental, numerical and analytical techniques. Lin *et al.* (2006, 2007) studied the fatigue life by an analytical technique. Lin *et al.* (2003) investigated the fatigue life of spot welds under combined loadings using analytical approaches. Pan and Sheri (2002, 2003) studied this process by means of a numerical simulation. They verified their results with experimental data. Zhang and Taylor (2000) studied the effects of thickness on the growth of crack fatigue. They found that the number of loading cycles for a complete fatigue depends on t^s, where t is the thickness of specimen and s, which is 0.5 approximately, is the property of material under loading. Deng *et al.* (2000) studied the effects of weld spot diameter and the plasticity of the welding material due to loading on the fatigue strength of the spot weld using a three dimensional simulation with a finite element method. Sevim (2006) studied the hardness of weld point materials on stress intensity factor. Bouyousfi *et al.* (2007) investigated the effects of different parameters in spot welding process on the strength of the nugget. Svenssona *et al.* (2005) studied the effects of cyclic loading with variable amplitude on the fatigue life of spot weld point. The aim for all of the investigations in this field is to predict the fatigue strength of a spot weld and to design and produce the spot weld specimens as accurately as possible. Lin and Pan (2008) used the closed-form stress intensity factor solutions in terms of structural stresses for the spot welds under various types of loading conditions. The results were obtained based on the theories of elasticity and fracture mechanics. Using the J integral for a strip model a closed-form of an analytical stress intensity factor solutions for spot welds joining two plates of equal thicknesses were derived in terms of the structural stresses around a rigid inclusion in a plate under various types of loadings. The closed-form solutions presented were used as the basis of developing a new analytical stress intensity factor solution for spot welds in various types of specimens presented in subsequent papers. Marashi *et al.* (2008) used the resistance spot welding techniques to join austenitic stainless steel and galvanized low carbon steel. The relationship between the

Corresponding Author: M. Shariati, Department of Mechanical, Shahrood University of Technology, Daneshgah Blvd. Shahrood, Islamic Republic of Iran Tel: +98(273)3332230 Fax: +98(273)3335600

failure mode and the weld fusion zone characteristics (size and microstructure) was studied. It was found that spot weld strength in the pullout failure mode was controlled by the strength and the fusion zone size of galvanized steel sides. The hardness of fusion zone which is governed by the dilution between two base metals and the fusion zone size of galvanized carbon steel side were found to be the dominant factors in determining the failure mode. Sun and Khaleel (2007) summarized the dynamic joint strength evaluation procedures and the measured dynamic strength data for some joint populations of Self-Piercing Rivets (SPR) and Resistance Spot Welds (RSWs) joined the similar and dissimilar metals. The majority of experimental results showed that joint strength increased with any increase in loading rate. It was also found that with any increase in loading velocity displacement to failure decreased for all joint samples. Therefore, brittleness of the joint sample increases with any impact velocity. Kong *et al*. (2008) studied a Resistance Spot-Welding (RSW) joint consisting several material zones with different microstructure and properties as a result of thermal, metallurgical and mechanical deformation processes. They used an inverse modeling methodology which combines a numerical modeling and indentation tests with a standard hardness to characterize the detailed properties of different weld zones of spot-welded joints. A 3-D finite element model based on the predicted constitutive material laws for different zones coupled with a fracture model was developed to predict the deformation of spot-welded joints beyond the onset of initial yield under tensile-shear loading. Microstructural characterization, microhardness tests, tensile shear tests and fatigue tests of spot-welded Hot Dipped Galvanized (HDG) DP600 steel were studied by Maa *et al*. (2008). The effects of weld expulsion on the microstructural characteristics, mechanical properties and fracture modes were investigated using optical microscopy, image analysis and Scanning Electron Microscopy (SEM) together with Energy Dispersive X-ray Spectroscopy (EDS). Fatigue tests showed a slight lower fatigue limit for the joints with the expulsion. Lotsberg (2008) obtained analytical expressions for stress concentration factors in pipes subjected to internal pressure and axial force for a number of design cases based on classical shell theory. The effect of fabrication tolerances in simple butt welds was assessed. Analyses based on classical mechanics were compared with results from axisymmetric finite element analyses for verification of the methodology. An analytical expression for the bending stress in the pipe wall due to this out-of-roundness was presented. The derived stress concentration factors could be used with a hot spot stress S-N curve to calculate the fatigue damage. Wang and De-Guang (2008) performed elasto-plastic finite element analysis for single spot welds in tensile shear loading using ANSYS software. According to the relationship between the micro-hardness and strength the cyclic material constants for different zones in the periphery of spot welds were determined in terms of hardness distribution and material fatigue parameters. The life prediction results showed that both equations were in good agreement with experimental data in low cycle fatigue life regime. Fatigue properties and the failure characterization of high strength spot welded steels were studied by Long and Khanna (2007). The tensile shear and coach peel samples were used in their investigation. Micro-hardnesses were measured to study the hardness change across the nugget weld. Under low and high loading cycles all the materials showed very similar fatigue strength. The crack initiation and propagation during the fatigue loading history have been experimentally determined and discussed. Lin *et al.* (2007) performed analytical solutions of the stress intensity factor in mode I for spot welds in lap-shear specimens based on the classical Kirchhoff plate theory for linear elastic materials. They derived a closed-form solution for an infinite plate containing a rigid inclusion under counter bending conditions. Using the J integral, the closed-form solutions were developed to obtain analytical solutions for the stress intensity factor in mode I for spot welds with large and finite sizes lap-shear specimens. The results based on the finite square plate model with an inclusion indicated that the stress intensity factor solution in mode I agreed well with the computational results for lap-shear specimens. Feulvarch *et al*. (2006) performed a fully coupled finite-element simulation and experimental approach to investigate the weld growth mechanisms in resistance spot welding. The experimental results were used to measure the interface contact properties in the finite element simulation. The experimental shape evolution of the nugget was compared well with the numerical results

In the current study the behavior of the crack growth, the fatigue life of TS specimens under different level of loadings and the determination of the plate thickness on the fatigue life are investigated by experiment.

MATERIALS AND METHODS

Three different types of Tensile Shear (TS) specimens with different thicknesses are used in this investigation. The dimension of specimens are shown in Fig. 1. As shown in the Fig. 1 the TS specimens with two plate thicknesses of 1 by 1 mm, 1 by 1.5 mm and 1.5 by 1.5 mm are weld jointed together. At least 5 specimens of each

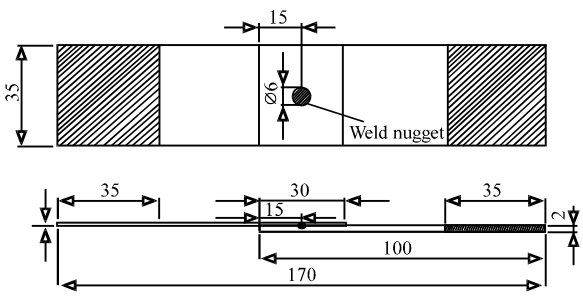

Fig. 1: Geometry and dimensions of a TS spot welded specimen

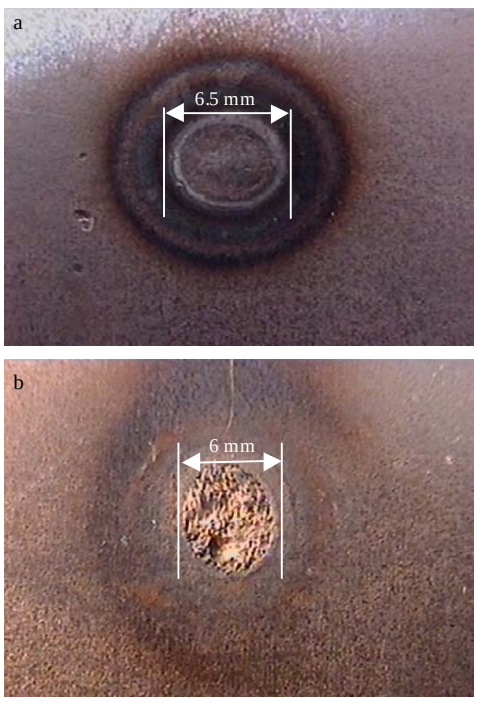

Fig. 2: (a) Spot weld cross section at plate surface (electrode diameter = 6.5 mm) and (b) Spot weld cross section at high load after failure (electrode diameter is 6 mm approximately)

Table 1: Shear strength in specimens

TS specimen (mm)	Shear strength (N)
1-1	5540
1-1.5	6650
1.5-1.5	9200

type under different loading with constant amplitude conditions are used. The fatigue life of specimens varies from 10,000 to 1,000,000 cycles.

Welding specimen's conditions: The specimen's were provided by means of a pedal spot welding apparatus.

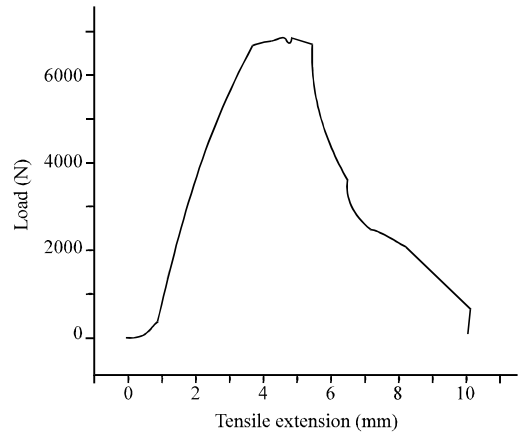

Fig. 3: Load versus displacement for TS:1-1.5 mm

The welding conditions are as follows:

Welding current = 8 kA
Welding time = 3 sec
Electrode diameter = 5.6-6 mm

Specimen's nomenclature: As plates with different thicknesses are used, TS specimens are classified into four different groups. All specimens are represented as TS **-**-* , where TS indicates the type of specimen. The first two digits indicate the thickness of plate multiplied by 10. The second two digits shows the thickness of the other plates multiplied by 10 and the last digit indicates the specimen's number in each series of the test. At least three specimens are used in the spot welding test.

Shear strength of spot welding: The diameter of nuggets were 6 mm (Fig. 2a, b). The shear strength of each specimen was measured in tensile test. The mean shear strength of specimen, which is the maximum tolerable shear force for the spot weld, are shown in Table 1.

An example of a measured shear load for a nugget is shown in Fig. 3.

MATERIAL PROPERTY

All specimens used in this study are made of st37 steel. The standard tensile tests of tension of metallic materials, E8, are performed to determine the stress-strain diagram according to ASTM standards. Two tensile tests were performed for each plate with 1 and 1.5 mm. Some of these measurements in form of load-displacement curves and stress-strain diagrams are shown in Fig. 4. The maximum tolerable force are found to be 4249 and

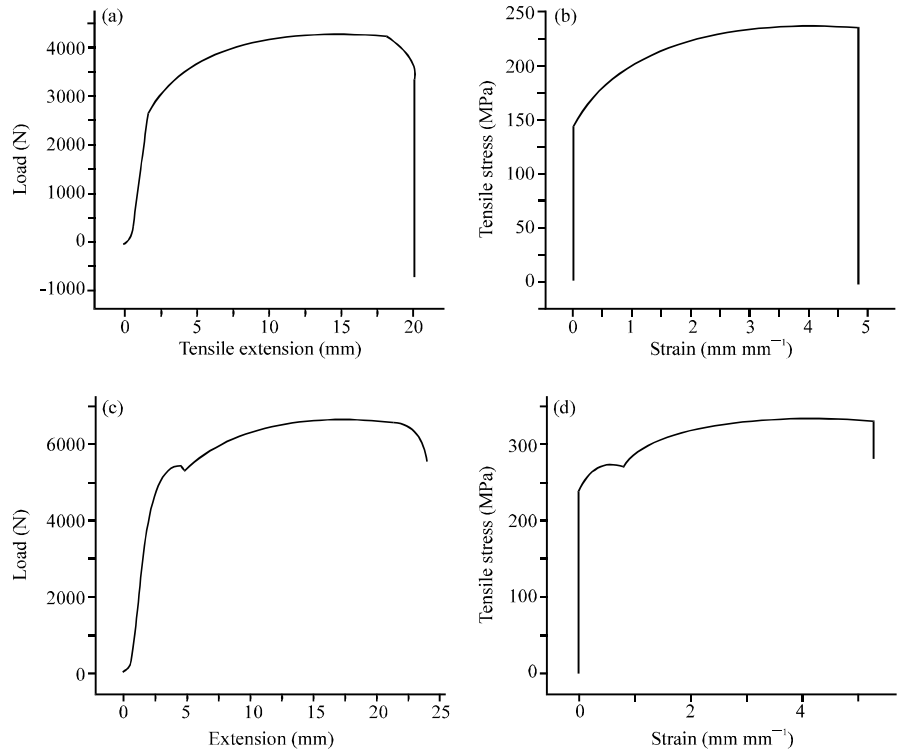

Fig. 4: (a) Load-displacement curve for 1 mm plate, (b) Stress-strain curve for 1 mm plate, (c) Load displacement curve for 1.5 mm plate and (d) Stress-strain curve for 1.5 mm plate

Table 2: Fatigue life for TS specimens with R = 0.01

Experimental observation	Load ratio (R)	Nt No. of loading cycles to failure	Maximum applied load (kN)	TS type
Plate tears about spot weld in specimen	0.01	197654	1.75	1-1 mm
Plate tears about spot weld in specimen	0.01	55608	2.00	
Relative tear also occur in other plate				
Plate tears about spot weld in specimen	0.01	20809	2.25	
Relative tears also occur in other plate				
Plate tears about spot weld in 1 mm plate	0.01	291641	1.75	1.5-1.5 mm
Width failure in 1 mm plate, no crack in other plate	0.01	271683	2.00	
Plate tears about spot weld in 1 mm plate	0.01	184992	2.25	
Plate tears about spot weld in 1 mm plate A 4 mm crack is observed in other plate	0.01	49915	2.50	
Width failure in specimen, a 20 mm crack is observed in other plate	0.01	636618	2.00	1.5-1.5 mm

5616 (N) for 1 and 1.5 mm plates, respectively. The width of specimens in theses standard tensile tests were 12.5 mm.

Fatigue tests

Fatigue life prediction: The fatigue tests were performed using a servo-hydraulic Instron 8802, as shown in Fig. 5, with constant amplitude loadings. The experimental results for each three specimen under the frequency of 10 Hz and the loading controlled conditions were performed. Table 2 shows the results for all three specimens.

The load versus the number of tolerable cycles is shown in Fig. 6 for each of the specimen.

The results of the fatigue test with frequency of 20 Hz, R = 0.05 and under the constant controlled loading conditions are shown in Table 3. In Fig. 7 the diagram of the load versus the fatigue life for each of the three specimens are shown. The life pertains to all of the three steps of fatigue as initiation, propagation and the failure of the fatigue for specimen.

Fatigue crack growth behavior: The most majority part of the fatigue life pertains to initiation, the crack growth at the spot weld and its propagation to the surface of a specimen which cannot be observed. Since the crack growth behavior can be studied exactly as it clearly appears at the surface, an optical microscope with

Fig. 5: Specimen's placement between fatigue test apparatus clamps (INSTRON 8802)

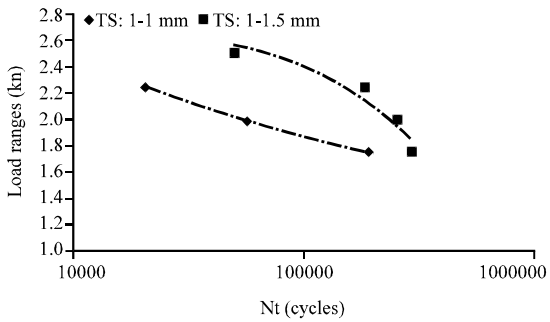

Fig. 6: Load-fatigue life curves for TS specimens with R = 0.01

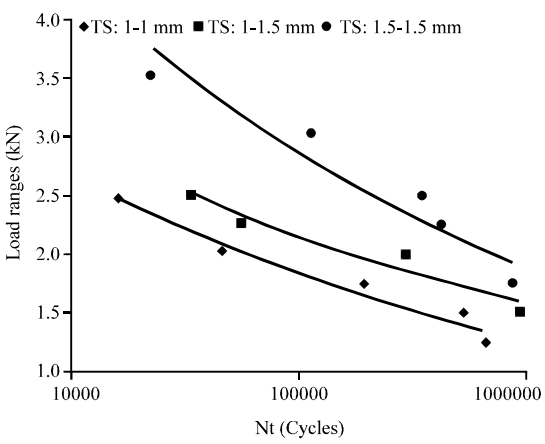

Fig. 7: Load-fatigue life curves for TS specimens with R = 0.05

magnification factor of 100 is used to measure the crack length, shown in Fig. 8, at different loading cycles. Prior reaching the crack to the specimen's surface, many small valleys can be observed around the spot weld due to the application of the loads and the deformation of the specimen.

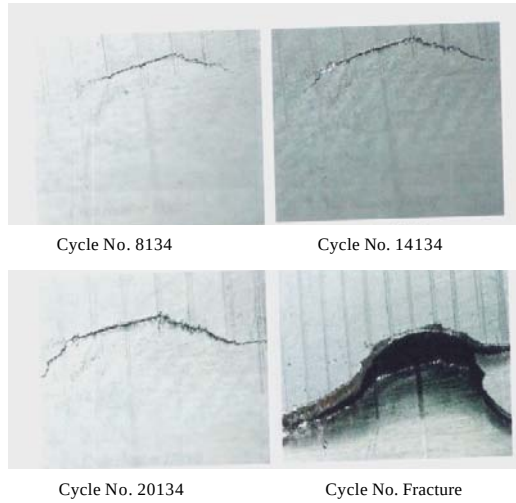

Fig. 8: Crack growth snapshots by optical microscopes at specimen's surfaces

Table 3: Fatigue results for TS specimens with R = 0.05

F_{max} (kN)	N_t = No. of cycles to complete failure N_t 1-1 : TS (mm)	1-1.5 : TS (mm)	1.5-1.5 : TS (mm)
1.25	659,222	---	---
1.50	524,428	943576	---
1.75	191,335	520,095	874,606
2.00	49,995	296,627	---
2.25	---	55,062	425,946
2.50	16,109	33,253	347,830
3.00	---	---	114,747
3.50	---	---	22,801

Table 4: Fatigue crack life during initiation, growth to surface and complete failure steps

TS specimen (mm)	N_t = Final life	N_p = Cycle at which the crack is visible at the specimen's surface	Maximum applied load (N)	100× (N_p/N_t)
1-1	197654	97865	1750	49.5
	55608	35000	2000	62.9
	20809	18938	2250	91.0
1-1.5	271641	140015	1750	51.5
	271683	200000	2000	73.6
	184982	102000	2250	55.1
	49915	29000	2500	58.1
1.5-1.5	636618	467161	2000	73.4

The crack life percentage and the number of loading cycles due to the initiation and the crack growth steps before reaching to the plate surface for different loading conditions and different thickness of TS specimens are given in Table 4 . The Table 4 reveals that:

- About 50 to 90% of the crack life relates to the initiation and the growth within specimens
- As the specimen's thickness increased, the life percentage in which the crack grows within the specimen also increased

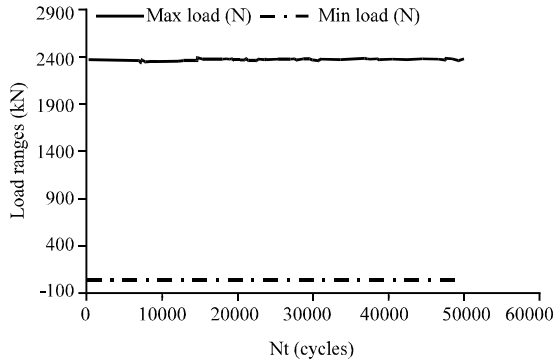

Fig. 9: Load versus number of loading cycles for TS10-15-4

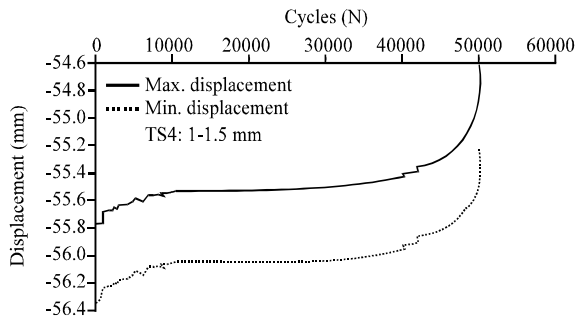

Fig. 10: Displacement-loading cycles for TS-10-15-4

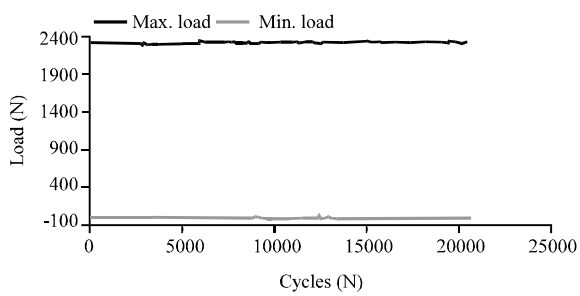

Fig. 11: Load versus cycles for TS-10-10-4

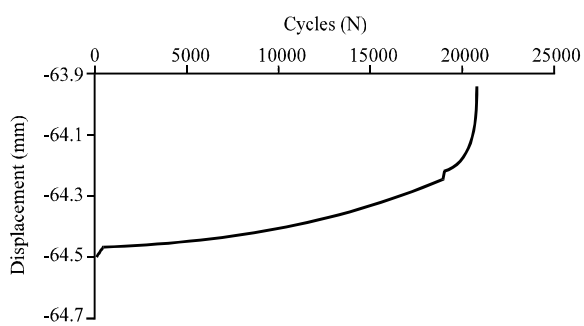

Fig. 12: Displacement-Cycles for TS10-10-4

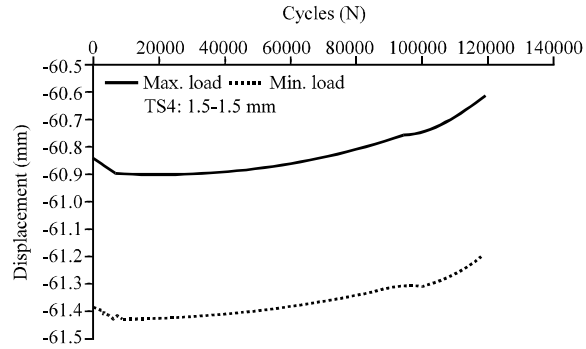

Fig. 13: Displacement-cycles curve for TS-15-15-4, Crack initiates at 38000, F_{max}=3 kN, R = 0.05

- As explained earlier the initiation and the crack growth within the specimen is impossible to measure unfortunately, however the initiation of the crack propagation within the specimen can be measured by monitoring the stiffness variations during the application of load. In other words, the diagram of load versus the number of loading cycles for specimen may be plotted from the beginning to the end of the loading and computing the global slope of the diagram. The crack growth initiation pertains to the points of diagram at which the slope rates are significant. At this point the number of cycles can be found. If this is subtracted from the number of cycles for the first crack observation at the specimen's surface, the number of loading cycles from the start of the crack propagation to the observation of the crack at the surface can be calculated. This is shown in Fig. 9-13, for TS 10-15-4 and TS 10-10-4 samples
- As shown in Fig. 10, the start of the crack propagation in TS-10-15-4 specimen occurs at 12,000 loading cycle at which the rate of displacement versus the loading cycles is approximately zero. The first observed crack at the surface of a thin specimen is detected at 29000 loading cycles

As shown in Fig. 14, the crack propagation initiates within TS10-10-4 specimen at 6000 loading cycles.

In Fig. 13-15 the number of loading cycles with respect to displacement are shown.

Some snapshots relating to TS-10-15-3's crack growth during observation at the surface and the final failure, taken by Nikon optical microscope with 100 magnification factor, are shown in Fig. 16.

Also snapshots relating to the TS10-15-2's crack growth during observation at the surface and the final

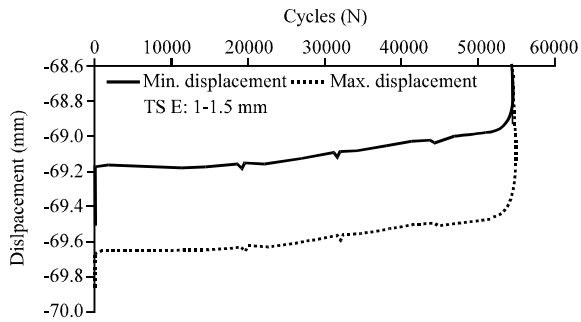

Fig. 14: Displacement-cycles curve for TS-10-15-E, Crack initiates at 21000, 0.05 = R, kN 2.25 = F_{max}

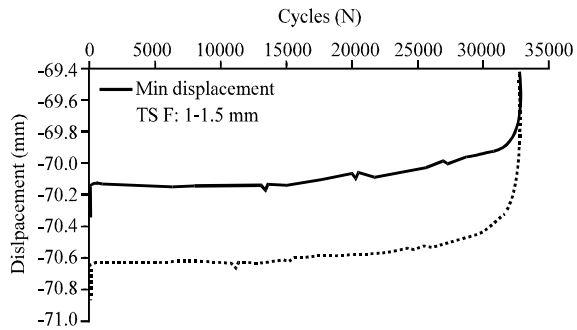

Fig. 15: Displacement-cycles curve for TS-10-15-F 0.05 = R, kN 2.5 = F_{max}

failure are shown in Fig. 17. Figure 17 reveal that complete failure occurs as quickly as the cracks are observed at the specimen's surface.

Figure 18 and 19 show the crack length versus the number of loading cycles for TS10-15-2 and TS10-15-1 specimens.

For both of the specimens the following relations between the crack length a and the number of loading cycles N are obtained.

For TS-10-15-2 :

$$a = 0.0773e^{2\times10^{-5}N}$$

For TS-10-15-2 :

$$a = 0.0683e^{9\times10^{-6}N}$$

The crack growth rate with respect to the loading cycles is obtained by differentiating the above formulas with respect to N.

$$\frac{da}{dN} = 0.154\times10^{-5}e^{2\times10^{-5}N}$$

$$\frac{da}{dN} = 0.596\times10^{-6}e^{9\times10^{-6}N}$$

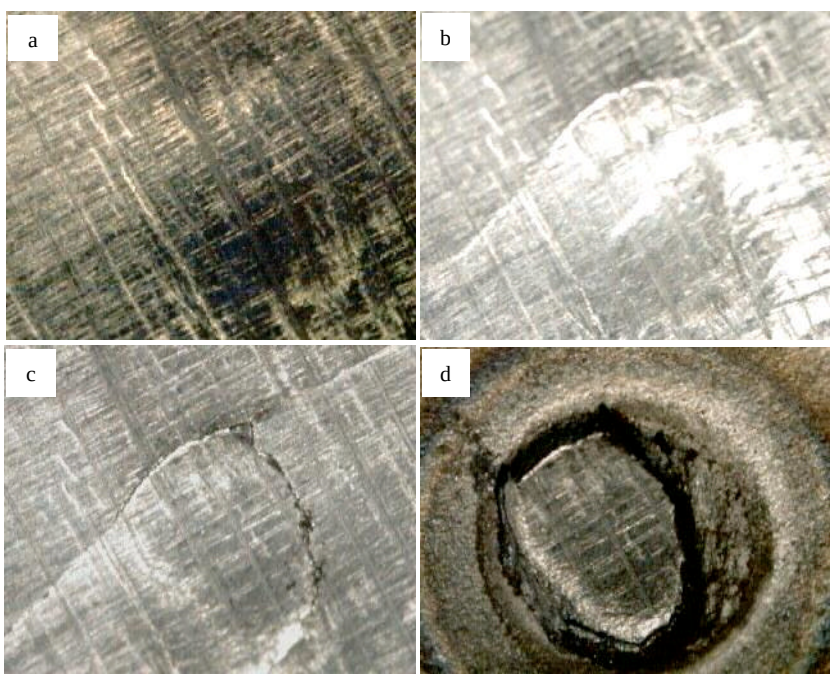

Fig.16: Stepwise snapshots for crack growth of spotweld during observation at surface and complete failure (a): Spotweld snapshot after 50000 loading cycles, (b): Spotweld snapshot after 160000 loading cycles, (c): Spotweld snapshot after 182000 loading cycles, (d): Spotweld snapshot after 184992 loading cycles

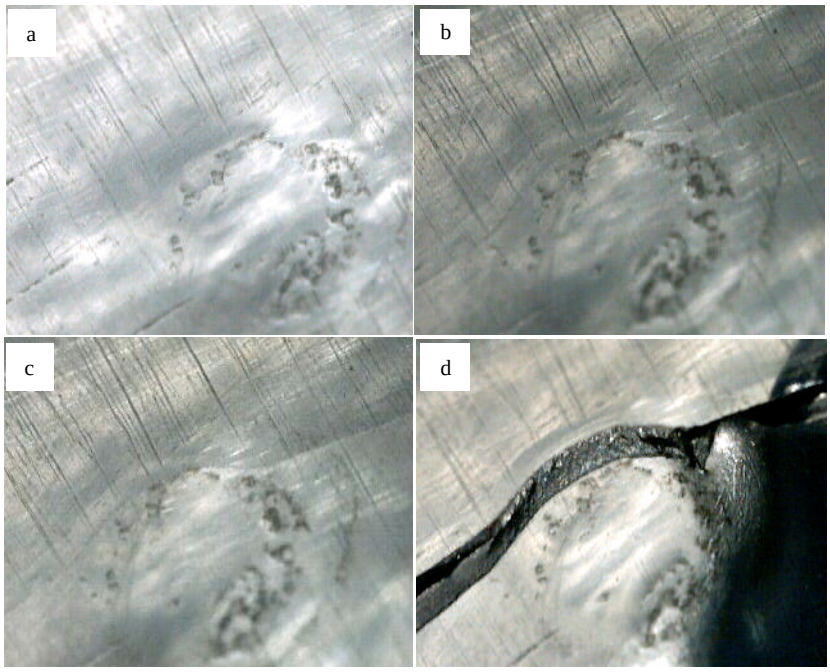

Fig. 17: Stepwise snapshots for crack growth of spotweld during observation at surface and complete failure (a): Spotweld snapshot after 50000 cycles, (b): Spotweld snapshot after 258000 cycles, (c): Spotweld snapshot after 271000 cycles, (d): Spotweld snapshot after 271673 cycles

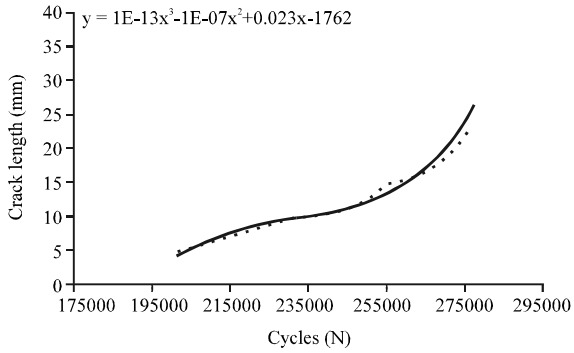

Fig. 18: Crack length versus cycles for TS10-15-2, F_{max}=2 kN

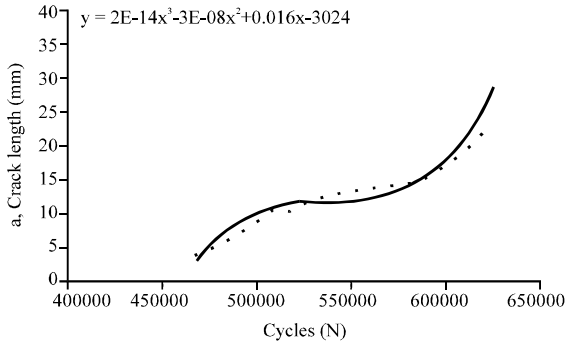

Fig. 19 : Crack length versus cycles for TS10-15-1

RESULTS AND DISCUSSION

As Fig. 20-21 show, the initiation and the crack growth for all specimen occur around the spotweld from the direction of loading applied.

Crack is always observed in thinner plate's and it's length is longer with respect to the thicker plate. This is shown in Fig. 22-23.

The crack lengths for both specimens are approximately equal for plates with constant thicknesses.

In low level loading conditions, crack initiates around the spotweld and propagates significantly in the direction of plate width and complete failure occurs finally (Fig. 24). As the loading increased the crack propagates much slower in plates than spotweld's regions. It finally pulled out the nugget and failure occurs as in Fig. 25.

In extreme loading conditions, the nugget is pulled out without any observation of the crack growth (Fig. 26).

Due to the stress concentration around the spotweld, crack always initiates around the nuggets with smallest distance to the edge of loading applied, grows 45-60 (degree) in the directions with approximately around the weld and propagates toward the external edge of the specimen (Fig.19-21).

Sometimes, when two plates are spot welded together, two opposite truncated conic shapes can be observed at the connections which are schematically shown in Fig. 27. The real connection is also shown in

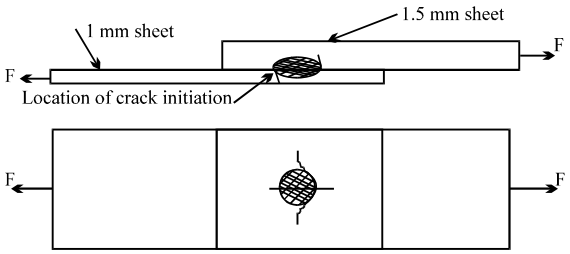

Fig. 20: Location of initiation and crack growth around a spotweld

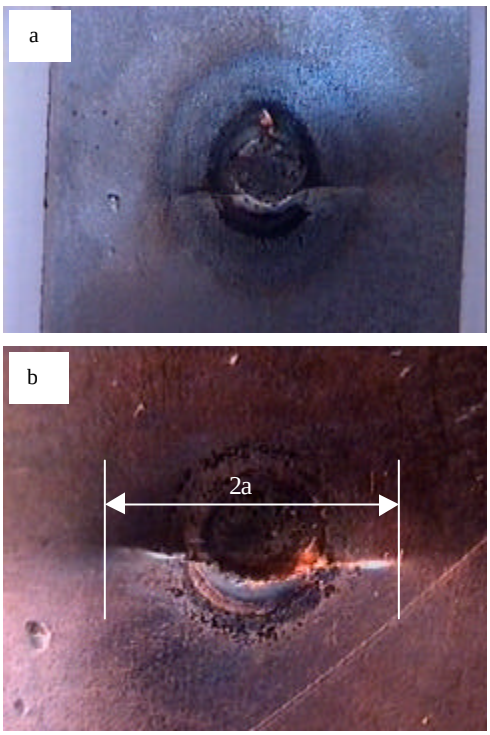

Fig. 21: Location of (a) initiation and (b) crack growth for a real specimen

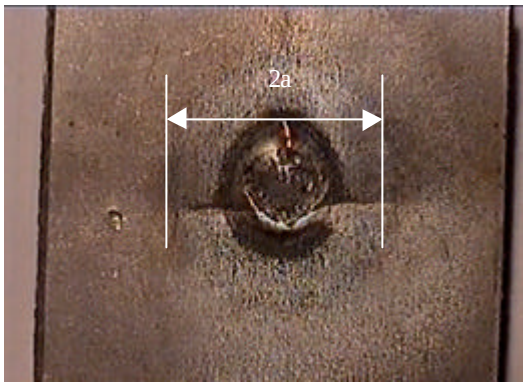

Fig. 22 : Crack length in 1 mm thick plate

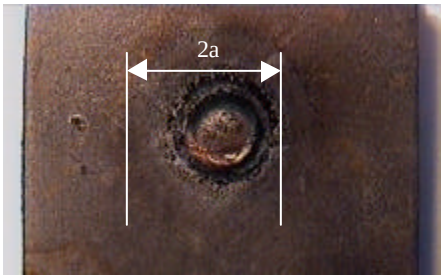

Fig. 23: Crack length in 1.5 mm thick plate

Fig. 24: Complete failure and crack propagation in plates subjected to low level of loadings

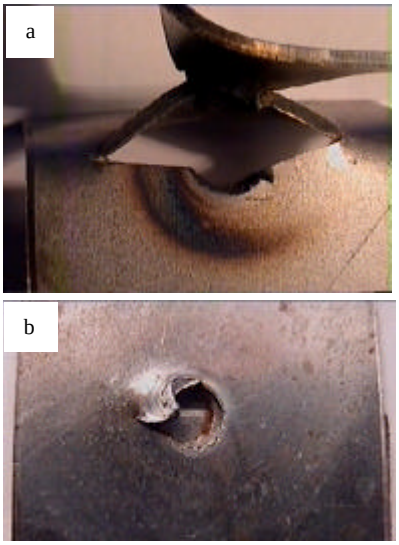

Fig. 25: (a) Crack propagation in plates subjected to high level of loadings and (b) failure occurs after a gradual growth

Fig. 26: Nugget pulled out on applying an extreme loading

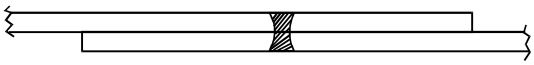

Fig. 27: A schematic representation of two truncated conics at spotweld connection

Fig. 28: Incomplete conic geometry of spotweld between two plates

Fig. 28 . This cause stress concentration at the welding point as wellas initiation and the crack growth at this point.

Crack initiates and grows at the location of two plate connections. Then it approaches to the specimen's surfaces and then propagates with relatively high speed.

CONCLUSION

Since in high level loadings, the nugget is pulled out after a small crack growth, the fatigue life of specimen decreased with any increase in loading. However, in low level loading, the crack grows significantly.

The initiation and the crack growth first occurs in TS specimen having small thicknesses in which the crack length is longer.

Since the failure requires the growth of the crack to the external surface of the specimen and the crack propagation along the width (Fig. 6, 7, Table 4), in thicker TS specimen, the fatigue life is longer. In Table 4 for example amongst the specimens with the same loading levels (N = 200) those with the higher thickness plates have much longer life. In other words, the fatigue life for TS 1.5-1.5 is longer than TS 1-1.5 and that of TS 1-1.5 is longer than TS 1-1's life.

Overloaded plates are suddenly fails without withstanding the fatigue loading and the nugget pulls up suddenly.

In Specimens with the same thicknesses, cracks are observed in both plates with an approximately the same length.

Due to stress concentration at the vicinity of the nugget, crack grows around it as an arc shape and failure normally occurs at the plate rather than the weld point.

The majority portion of the fatigue life of spot welds relates to the initiation and the crack growth to the specimen's surface. This is about 50-91% as shown in Table 4.

In spot welds with different thicknesses, the fatigue life does not change significantly. In other words, the fatigue life in spot welding of a 1 mm plate to plate with 1 and 2 mm thicknesses are approximately the same as the failure occurs in thinner plates (1 mm plate).

Research in this field can be extended to study the followings:

- The fatigue life of weld points subjected to random or impact loadings
- Experiments on real specimens with more complicated geometries and loadings
- Experiments on specimens having the same material as in an automobile bodies

REFERENCES

Bouyousfi, B., T. Sahraoui, S. Guessasma and K.T. Chaouch, 2007. Effect of process parameters on the physical characteristics of spot weld joints. Mater. Design, 28: 414-419.

Deng, X., W. Chen and G. Shi, 2000. Three-dimensional finite element analysis of the mechanical behavior of spot welds. Finite Elements Anal. Design, 35: 17-39.

Feulvarch, E. P. Rogeon, P. Carre, V. Robin, G. Sibilia and M. Bergheau, 2006. Resistance spot welding process: Experimental and numerical modeling of the weld growth mechanisms with consideration of contact conditions. Numerical Heat Transfer, Part A., 49: 345-367.

Kong, X., Q. Yang, B. Li, G. Rothwell, R. English and X.J. Ren, 2008. Numerical study of strengths of spot-welded joints of steel. Mater. Desig., 29: 1554-1561.

Lin, S.H., J. Pan, S.R. Wu, T. Tyan and P. Wung, 2002. Failure loads of spot welds under combined opening and shear static loading conditions. Int. J. Solids Struct., 39: 19-39.

Lin, S.H., J. Pan, T. Tyan and P. Prasad, 2003. A general failure criterion for spot welds under combined loading conditions. Int. J. Solids Struct., 40: 5539-5564.

Lin, P.C., S.H. Lin and J. Pan, 2006. Modeling of failure near spot welds in lap-shear specimens based on a plane stress rigid inclusion analysis. Eng. Fract. Mech., 73: 2229-2249.

Lin, P.C., D.A. Wang and J. Pan, 2007. Mode I stress intensity factor solutions for spot welds in lap-shear specimens. Int. J. Solids Struct., 44: 1013-1037.

Lin, P.C. and J. Pan, 2008. Closed-form structural stress and stress intensity factor solutions for spot welds under various types of loading conditions. Int. J. Solids Struct., 45: 14-15.

Long, X. and S.K. Khanna, 2007. Fatigue properties and failure characterization of spot welded high strength steel sheet. Int. J. Fatigue, 29: 879-886.

Lotsberg, I., 2008. Stress concentration factors at welds in pipelines and tanks subjected to internal pressure and axial force. Marine Struct., 21: 138-159.

Maa, C., D.L. Chen, S.D. Bhole, G. Boudreau, A. Lee and E. Biro, 2008. Microstructure and fracture characteristics of spot-welded DP600 steel. Mater. Sci. Eng., A485: 334-346.

Marashi, P., M. Pouranvari, S. Amirabdollahian, A. Abedi and M. Goodarzi 2008. Microstructure and failure behavior of dissimilar resistance spot welds between low carbon galvanized and austenitic stainless steels. Mater. Sci. Eng., A480: 334-346.

Pan, N. and S. Sheri, 2002. Spot welds fatigue life prediction with cyclic strain range. Int. J. Fatigue, 24: 519-528.

Pan, N. and S.D. Sheri, 2003. Stress intensity factors in spot welds. Eng. Fract. Mech., 70: 671-684.

Sevim, I., 2006. Effect of hardness to fracture toughness for spot welded steel sheets. Mater. Design, 27: 21-30.

Sun, X. and M.A. Khaleel, 2007. Dynamic strength evaluations for self-piercing rivets and resistance spot welds joining similar and dissimilar metals. Int. J. Impact Eng., 34: 1668-1682.

Svenssona, T., P. Johannessona and Jacques de Maré, 2005. Fatigue life prediction based on variable amplitude tests-specific applications. Int. J. Fatigue, 27: 966-973.

Wang, R.J. and S. De-Guang, 2008. Low cycle fatigue life prediction of spot welds based on hardness distribution and finite element analysis. Int. J. Fatigue. 10.1016/j.ijfatigue.2008.04.009

Zhang, Y. and D. Taylor, 2000. Sheet thickness effect of spot welds based on crack propagation. Eng. Frac. Mech., 67: 55-63.